

Wavelets On Optimal Sampling Lattices for Volumetric Data

Alireza Entezari

Niklas Röber

Torsten Möller

Graphics, Usability, and Visualization (GrUVi) Lab, School of Computing Sciences, Simon Fraser University

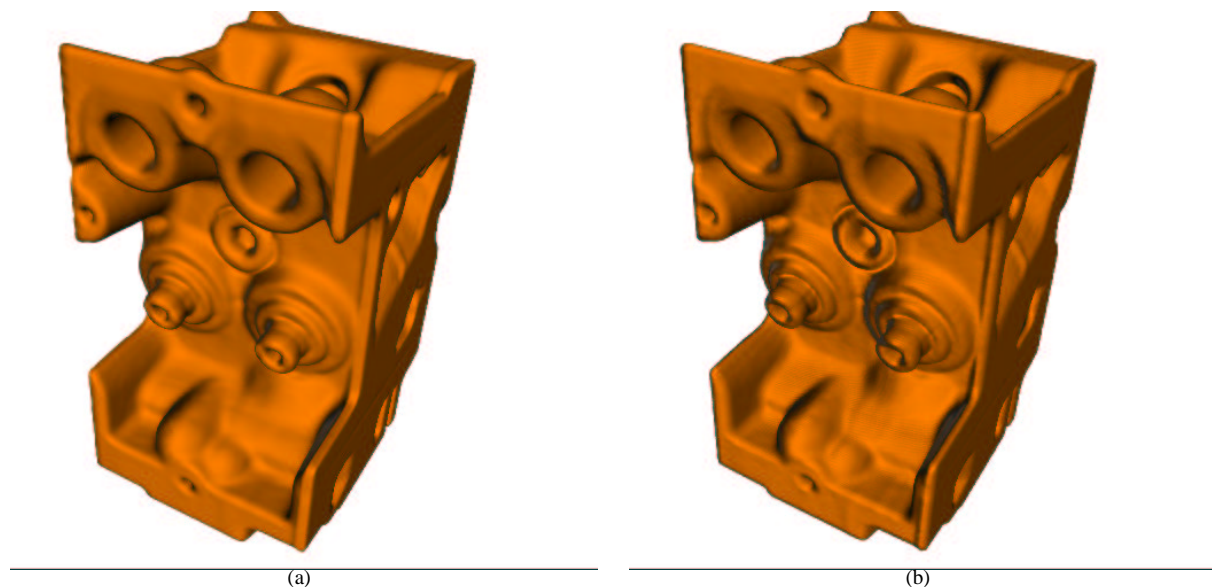


Figure 1: Engine, separable subsampling, smooth (left) and our non-separable subsampling, more detailed (right). An examination of the original data set in Figure 4 reveals the high fidelity of our subsampling method.

ABSTRACT

We exploit the theory of optimal sampling lattices in designing wavelets and filter banks for volumetric datasets. A true multidimensional (non-separable) filter bank is derived for the case of Haar wavelets and applied to various datasets for comparison with the corresponding separable multidimensional method. We propose a non-separable wavelet transform that yields the subsampled data on an optimal sampling lattice. This new non-separable filter bank allows for more accurate and efficient multi-resolution representation of the data over the traditional separable transforms. Furthermore, we take advantage of methods that render the data directly from this optimal sampling lattice to get images that demonstrate the superior quality of the subsampled data of our new algorithm compared to traditional methods.

CR Categories: K.6.1 [Computer Graphics]: Volumetric Data—Hexagonal sampling K.7.m [Multidimensional Signal Processing]: Filter Banks—Wavelets

Keywords: Body Centered Cubic lattice, Wavelets, Multiresolution, Multidimensional Signal Processing, Optimal Sampling, Volumetric Data

1 INTRODUCTION

Sampling theory has received a lot of attention as digital signal processing technology evolves. Usually we are processing and dealing with continuous phenomena, such as audio signals in 1D, images in 2D and medical images in 3D. However, our digital computers need to work with a finite set of samples from the continuum. Regular sampling is widely used since it can be described merely by a set of basis vectors [5]. In effect, we evaluate the continuous function at points in space which are integer linear combination of the basis vectors. Lattices are the corresponding mathematical abstraction of regular sampling. A lattice is described by a matrix called the *sampling matrix*; the sampling matrix is simply formed by the basis vectors of the sampling operation as its columns. If the sampling matrix of a sampling scheme is a diagonal matrix, that scheme is called separable otherwise it is called non-separable.

Separable sampling methods are the common choice due to their simplicity and the ability to treat each dimension independently. This has led to the commonly known Cartesian lattices. However, non-separable sampling methods have been proven to be more efficient under several different constraints. Hexagonally based sampling lattice has been proven to be the most optimal sampling lattice for the most general applications in signal processing [[2] [8]].

While there have been several algorithms to render one type of optimal regular grid - the so called Body-Centered Cubic (BCC)

[[1] [9]], there has been very little investigation on how to manipulate data on these lattices. In this paper we will present an algorithm for the creation of a multi-resolution pyramid on optimal regular lattices, such as the BCC lattice.

Due to simplicity, today's 3D scanners obtain samples on a Cartesian lattice; hence all of the existing real datasets that are captured by various modality scanners are sampled on the Cartesian lattice. For this reason, the algorithm proposed in this paper operates directly (without any re-sampling step) on the Cartesian lattice. Our proposed non-separable filter bank has been designed in a manner that creates the subsampled data on an optimal BCC lattice from a given Cartesian lattice. Hence, this method preserves more frequencies with the same amount of samples in comparison with the commonly used separable subsampling.

Another advantage of using non-separable wavelets is the flexibility that they offer in terms of filter design. When designing wavelets, it is desired that the basis functions be orthogonal and have linear phase. Nonetheless, it has been proven that achieving these two goals in one solution is impossible when designing one dimensional wavelets with higher order than the Haar wavelets. While the separable methods suffer from this restriction, non-separable wavelets in multi-dimensions can achieve both orthogonality and linear phase in one solution [6].

While previous methods struggle to demonstrate the superiority of hexagonal sampling due to the lack of hexagonally acquired data [[8] [1] [9]], we are able to demonstrate that our hexagonally subsampled data is in all cases superior in quality to the Cartesian data of the same size obtained through a comparable algorithm. Furthermore our proposed non-separable subsampling method is computationally more efficient than equivalent separable methods.

In Section 2 we summarize previous work in the fields of wavelet design and optimal sampling. Section 3 introduces the idea of non-separable subsampling which is followed by a wavelet filter design in Section 4. Section 5 shows the details of our algorithmic implementation, and our results follow in Section 6. We conclude our paper in Section 7 with a summary of our results and future research.

2 RELATED WORK

Optimal sampling structures have recently received a lot of attention in the field of volume rendering. [8] discusses the use of one of the optimal sampling lattices for volumetric data, called Body Centered Cubic (BCC) lattice. They illustrate the efficiency of this sampling lattice by comparing the quality of images rendered from the original data sampled on a Cartesian lattice with resampled data on a BCC lattice. During the resampling process they increase the sampling distance so that the BCC sampled volume has about 30% less samples yet still represents the same frequency spectrum as the original data on the Cartesian lattice. While there are visible differences it is inconclusive which one is superior in quality. One has to keep in mind, that the sampling artifacts for the BCC lattice will play a non-trivial role.

The BCC sampling lattice contains sampling points on a regular cube plus an extra sample in the center of the cube as illustrated in Figure 2.

The BCC sampling lattice can be described by the basis vectors that are the columns of the BCC sampling matrix:

$$V_{bcc} = \begin{bmatrix} T_b & -T_b & T_b \\ -T_b & T_b & T_b \\ T_b & -T_b & T_b \end{bmatrix}$$

where T_b is the sampling distance along each axes. Similarly, the Cartesian sampling lattice can be described by the basis vectors that

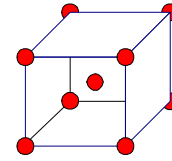


Figure 2: The BCC sampling lattice

are the columns of the Cartesian sampling matrix:

$$V_{cc} = \begin{bmatrix} T_c & 0 & 0 \\ 0 & T_c & 0 \\ 0 & 0 & T_c \end{bmatrix}$$

where T_c is the sampling distance for the Cartesian sampling lattice. Under the assumption of spherically band-limited data, Theufl et al [8] showed that using the BCC sampling lattice one can increase the BCC sampling distance T_b by $\sqrt{3/2}$ without creating any aliasing. This means that almost 30% less samples on the BCC lattice are just enough to preserve the high frequencies that exist in the original data.

Hence we conclude that the BCC lattice is a much more efficient lattice for capturing a signal than the Cartesian lattice. In fact, when we obtain the exact same number of samples using a BCC lattice and a Cartesian lattice, BCC sampled data preserves more details (higher frequencies) of the original data when compared to Cartesian sampled data. This amounts to a higher quality subsampling of the original data source, assuming we are able to use the same amount of data for Cartesian as well as for BCC data. This is the main motivation of our work throughout this paper.

The theory of subsampling has been previously studied in the signal processing community mainly for image processing applications. The theory has also been developed for higher dimensional signals [[17] [6] [13]]. However, the application of multidimensional subsampling has been focused on digital video processing where the time axes is treated as the third dimension of the signal [[7] [18] [19]]. A concern raised in the application of three-dimensional signal processing of digital video is that the third axes differs from the first two axis. In other words, the way data is distributed along the time axes is uncorrelated with the way data is distributed along X and Y axis. This issue remains as the main disadvantage of applying three-dimensional subsampling to video signals. However, volumetric data is a perfectly suitable application area of the optimal subsampling methods since we are dealing with a true three-dimensional signal.

Before the use of BCC data can be accepted by the mainstream, efficient rendering techniques need to be established. Theufl et al [8] have adapted splatting to render BCC data. Since splatting is an inherent blurry technique it comes as no surprise that the resulting images were blurry. Neophytou et al [9] adapted Shear-Warp to three-dimensional BCC lattice and four-dimensional D_4^* lattice with great results. Carr et al [1] have introduced efficient iso-surface extraction algorithm on BCC data and have analyzed their quality and efficiency. However, up to this date no "real" BCC data has been available in order to put these algorithms to a test. This paper will provide such data. Currently we are also developing algorithm for the rendering of BCC grids using texturing hardware. While these algorithms have been used for some of the renditions in this paper, we refer the interested reader to Röber et al [10].

3 SUBSAMPLING MATRIX

Wavelet decomposition in 3D is usually obtained through a tensor product of 1D wavelets; i.e. the wavelet decomposition is applied

along each axis in the signal (separable wavelets). Our contribution in this paper is to derive a perfect reconstruction filter bank that subsamples the 3D Cartesian sampled data in a non-separable fashion resulting in subsamples that are located on Body Centered Cubic lattice. This means that during the subsampling process we preserve as many high frequencies as theoretically possible due to the close packing achieved by the BCC lattice.

In one dimensional signal processing, a subsampling operation is defined as $y[n] = x[s \cdot n]$ where s is an integer denoting the ratio of the number of total samples to the samples preserved, x is the original signal and y is the signal after subsampling. This equation in higher dimensional spaces still holds, with the difference that the scalar s turns into a subsampling matrix D which is a square matrix of full rank and its size is the same as the dimensionality of the problem. The columns of this matrix are the basis vectors representing the lattice. Let \mathbf{n} be an integer vector, then the subsampling operation is defined as:

$$\mathbf{y}[\mathbf{n}] = \mathbf{x}[D\mathbf{n}] \quad (1)$$

This sampling matrix is represented on the lattice by a *fundamental parallelepiped*, which is formed by the basis vectors (columns of D). The subsampling process partitions the signal into copies of the fundamental parallelepiped that tile the entire signal space. It then replaces every parallelepiped with one sample. The fundamental parallelepiped for the 2D subsampling matrix

$$D = \begin{bmatrix} 1 & 1 \\ 2 & -2 \end{bmatrix} \quad (2)$$

is illustrated in red in Figure 3.

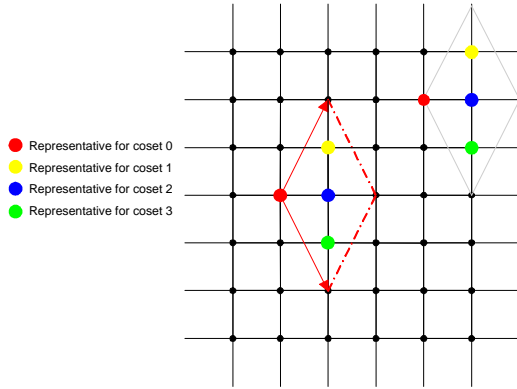


Figure 3: Subsampling using sampling matrix D in Equation 2

Analogous to the 1D example where every s samples are replaced by one sample, in the multidimensional case every $N = |\det D|$ samples are replaced by one sample. These N samples are contained in one fundamental parallelepiped formed by the subsampling matrix.

Instead of simply replacing N samples with one that is picked from the samples to be replaced (as indicated in Equation 1), we typically want to filter the data first (smoothing). This technique is basically a wavelet decomposition of the signal. For designing wavelet filters in multidimensional signal processing, we need to find filter coefficients h_n and a function $\psi(\mathbf{x})$ that satisfy the dilation equation using the subsampling matrix D :

$$\psi(\mathbf{x}) = \sum_{\mathbf{n}} h_{\mathbf{n}} \psi(D\mathbf{x} - \mathbf{n}) \quad (3)$$

As discussed in Section 4 perfect reconstruction filter banks have close ties with wavelet transforms. We compute the corresponding wavelet transform by designing a perfect reconstruction filter bank and iterating on its lowpass band signal.

3.1 Coset Analysis

A subsampling matrix D , reduces the signal cardinality by:

$$N = |\det D| \quad (4)$$

This is true regardless of the dimensionality of the signal since the volume of the fundamental parallelepiped is $\det D$ and the subsampling process replaces every parallelepiped with one sample. Every sample inside the fundamental parallelepiped belongs to a *coset*. A coset is the set of all sample points in the signal that rest on the same relative position within the fundamental parallelepiped on all of the copies of the fundamental parallelepiped throughout the signal. Roughly speaking one could compare the cosets to all possible “remainder” terms after a “division” by D . Since there are N samples inside the fundamental parallelepiped, there are N cosets. Every coset is represented by a vector from the origin to the position of the sample in the fundamental parallelepiped. Figure 3 demonstrates different locations inside two of the fundamental parallelepipeds with different colors; the samples belonging to the same coset have the same color. By inspection, the vectors representing the cosets in Figure 3 are:

$$\mathbf{k}_0 = \begin{bmatrix} 0 \\ 0 \end{bmatrix}, \mathbf{k}_1 = \begin{bmatrix} 1 \\ 1 \end{bmatrix}, \mathbf{k}_2 = \begin{bmatrix} 1 \\ 0 \end{bmatrix}, \mathbf{k}_3 = \begin{bmatrix} 1 \\ -1 \end{bmatrix}$$

Coset analysis has very close ties to the polyphase analysis discussed in Section 4.1. Because of this close relationship, in order to design perfect reconstruction filter banks, we need an algorithm to find the cosets of a subsampling matrix.

The coset vectors, satisfy the division theorem in vector arithmetic. This means that they are valid remainders in the division: $\mathbf{n} = D\mathbf{m} + \mathbf{k}_x$ where $0 \leq x < N$. Therefore, we can find the unique coset vectors for every subsampling matrix. Let $\mathbf{v}_1, \mathbf{v}_2, \dots, \mathbf{v}_d$ represent the basis vectors of the subsampling lattice (columns of D). Then, every sample point in the underlying lattice with coordinates \mathbf{n} can be expressed as $\mathbf{n} = \sum_{i=1}^d c_i \mathbf{v}_i$. Then, according to Cramer’s rule we have:

$$c_i = \frac{\det[\mathbf{v}_1 \cdots \mathbf{v}_{i-1} \mathbf{n} \mathbf{v}_{i+1} \cdots \mathbf{v}_d]}{\det[\mathbf{v}_1 \cdots \mathbf{v}_{i-1} \mathbf{v}_i \mathbf{v}_{i+1} \cdots \mathbf{v}_d]} = \frac{\det[\mathbf{v}_1 \cdots \mathbf{v}_{i-1} \mathbf{n} \mathbf{v}_{i+1} \cdots \mathbf{v}_d]}{N}$$

Since the \mathbf{v}_i ’s and \mathbf{n} are all integer vectors and the determinant of an integer matrix is an integer, every c_i is a rational number. Therefore, every c_i has an integer part a_i and a fractional part f_i which is a rational positive number less than one. The vector $\mathbf{a} = [a_1 \cdots a_d]^t$ denotes the fundamental parallelepiped that the sample at \mathbf{n} resides in; the vector $\mathbf{f} = [f_1 \cdots f_d]^t$ determines which coset this sample belongs to. For each fractional part we have: $f_i = \frac{x}{N}$ where $0 \leq x < N$. Therefore, we can determine all coset vectors by a linear combination of the basis vectors \mathbf{v}_i with the fractional numbers $g_i = \frac{x}{N}$ where $0 \leq x < N$. If the vector $\mathbf{k} = D\mathbf{g}$ is an integer vector, then the vector \mathbf{k} is a coset vector.

3.2 BCC Subsampling

The Body Centered Cubic lattice is described in [8] by :

$$V_{bcc} = \begin{bmatrix} 1 & -1 & 1 \\ -1 & 1 & 1 \\ 1 & 1 & -1 \end{bmatrix}$$

Our objective is to design a perfect reconstruction filter bank that uses the BCC matrix \mathbf{V}_{bcc} for subsampling and computes the wavelet transform of the signal as in Equation 3. However, this matrix is not suitable for satisfying the dilation equation. A necessary condition for a matrix to satisfy the dilation equation is that the absolute value of all of its eigen-values be strictly greater than one [6]. However, the eigen-values of this sampling matrix are: $\lambda_1 = 2.0$, $\lambda_2 = -2.0$, $\lambda_3 = 1.0$. This sampling matrix is not suitable for dilation since $\lambda_3 = 1.0$ and no dilation is obtained in one dimension while the other two dimensions dilate. To be more precise, when subsampling by \mathbf{V}_{bcc} , the axis along the third eigen-vector does not participate in the dilation process.

Moreover, in order to obtain a multiresolution scheme so that the geometric proportions of the objects in the lower resolutions are preserved, we need to dilate equally along all three axes. Hence, we desire equal eigen-values. Fortunately there is more than one matrix that describes the same sampling lattice [17]. In fact, all matrices that are obtained by multiplying \mathbf{V}_{bcc} with an integer unimodular matrix \mathbf{E} (i.e. $\det \mathbf{E} = 1$) represent the same lattice, they only index the samples differently.

We designed a procedure to search the space of all 3×3 integer triangular matrices \mathbf{E} with the diagonal elements being 1 or -1:

$$\mathbf{E} = \begin{bmatrix} (-1)^i & a & b \\ 0 & (-1)^j & c \\ 0 & 0 & (-1)^k \end{bmatrix}$$

where $i, j, k \in \{0, 1\}$ and $a, b, c \in \{0, \pm 1, \pm 2\}$. It is easy to see that \mathbf{E} is a unimodular matrix. We checked the product $\mathbf{E} \times \mathbf{V}_{bcc}$ for its eigen-values. If the absolute value of all eigen-values are equal and strictly greater than one, then the corresponding matrix \mathbf{E} would be a candidate unimodular matrix. We picked the candidate with the smallest elements since its fundamental parallelepiped is the least sheared. As a result we obtain

$$\mathbf{D} = \begin{bmatrix} -1 & 1 & 0 \\ 0 & 1 & 0 \\ 0 & 0 & -1 \end{bmatrix} \times \mathbf{V}_{bcc} = \begin{bmatrix} -1 & 0 & -1 \\ 1 & 0 & -1 \\ -1 & 2 & 1 \end{bmatrix} \quad (5)$$

This matrix is perfectly suitable for our dilation equation since $|\lambda_1| = |\lambda_2| = |\lambda_3| = 4^{1/3}$. Moreover, we obtain $\mathbf{D}^3 = 4^3 \mathbf{I}$. Indeed, after applying the down-sampling matrix \mathbf{D} once we convert a Cartesian lattice to a BCC lattice. After applying \mathbf{D} a second time (\mathbf{D}^2) we create the samples on another lattice called Face Centered Cubic (FCC). This lattice is another optimal sampling lattice which is the reciprocal of the BCC lattice [8]. Finally, after three applications of our down-sampling matrix \mathbf{D} we end up on a separable Cartesian lattice again. Hence, we can recursively run the downsampling process and compute the wavelet transform through iterating on the lowpass band of the filterbank. This is described in detail in Section 4. The vectors representing the cosets of this matrix are:

$$\mathbf{k}_0 = \begin{bmatrix} 0 \\ 0 \\ 0 \end{bmatrix}, \mathbf{k}_1 = \begin{bmatrix} 0 \\ 0 \\ 1 \end{bmatrix}, \mathbf{k}_2 = \begin{bmatrix} -1 \\ 0 \\ 0 \end{bmatrix}, \mathbf{k}_3 = \begin{bmatrix} -1 \\ 0 \\ 1 \end{bmatrix} \quad (6)$$

4 WAVELETS AND FILTER BANKS

Wavelet theory has been a popular theory in applied mathematics due to its flexibility and wide range of applications in various fields. The main advantage of wavelet analysis in comparison to Fourier analysis is its locality property. While Fourier analysis merely states which high frequencies exist in the signal, wavelet analysis tells us *where* those high frequencies exist in the signal. Due to this locality property of the wavelet basis, wavelet analysis

has been widely applied to image and signal processing for compression [11] and noise reduction [12].

Daubechies [4] showed the close relation between the wavelet theory and perfect reconstruction filter banks. She showed that using an iterative method on the low pass band of a filter bank one can obtain the wavelet transform of the signal. In order to compute the wavelet transform which corresponds to a down-sampling matrix \mathbf{D} , we design a filter bank that uses \mathbf{D} for its subsampling operators and define the filtering operations accordingly. In this section we design filters to satisfy the dilation in Equation 3 for a downsampling matrix that results in a BCC lattice.

The polyphase domain analysis in the Z -domain has been found particularly useful for designing perfect reconstruction filter banks. Polyphase analysis is in direct relation to the coset analysis in Section 3.1. In fact, every phase of the signal or the filter corresponds to one coset of the signal or the filter. Polyphase analysis is particularly useful since it partitions the set of samples into subsets each of which is shift-invariant with respect to the sampling operation; in other words, a delayed signal in one phase will still be in the same phase. This helps us to divide the big task of filter design for a shift-variant signal to several smaller problems of filter design for shift-invariant signals. Similarly, we represent the filter in the polyphase domain.

For the subsampling matrix \mathbf{D} we define the polyphase transform ¹ of the signal as:

$$X(z) = \sum_{\mathbf{k}_i \in \mathcal{U}_c^t} z^{\mathbf{k}_i} X_i(z^{\mathbf{D}}) \quad (7)$$

Here, \mathcal{U}_c^t denotes the set of coset vectors of the transpose subsampling matrix, \mathbf{D}^t , $X_i(z)$ denotes the i^{th} polyphase component of the signal:

$$X_i(z) = \sum_{\mathbf{n} \in \mathcal{Z}^n} x(\mathbf{D}\mathbf{n} - \mathbf{k}_i) z^{-\mathbf{n}}, \mathbf{k}_i \in \mathcal{U}_c^t \quad (8)$$

We define $\mathbf{p}_i(z) = [z^{\mathbf{k}_1} \dots z^{\mathbf{k}_N}]^t$, $\mathbf{k}_i \in \mathcal{U}_c^t$ to be the inverse polyphase transform vector and $\mathbf{x}_p(z) = [X_1(z) \dots X_N(z)]^t$ is the vector containing the polyphase components of the input signal. Then Equation 8 can be rewritten as:

$$X(z) = \mathbf{p}_i(z) \cdot \mathbf{x}_p(z^{\mathbf{D}}) \quad (9)$$

Moreover, the polyphase decomposition of a filter H , is defined as the vector of H_i 's:

$$H(z) = \sum_{\mathbf{k}_i \in \mathcal{U}_c^t} z^{-\mathbf{k}_i} H_i(z^{\mathbf{D}})$$

$$H_i(z) = \sum_{\mathbf{n} \in \mathcal{Z}^n} h(\mathbf{D}\mathbf{n} + \mathbf{k}_i) z^{-\mathbf{n}}, \mathbf{k}_i \in \mathcal{U}_c^t$$

Notice that the polyphase components of signals and filters are defined in a reverse fashion so as to account for the action of convolution [6].

The filter bank has several filters each of which is a band pass for a certain part of the frequency distribution of the signal. Each one of these filters has a polyphase expansion in the form of a vector. The matrix formed by vectors of all of the filters in the analysis bank of the filter bank is called *polyphase matrix* and denoted by $\mathbf{H}_p(z)$. The polyphase matrix for the synthesis bank is denoted by $\mathbf{G}_p(z)$. The overall filter bank equation in the Z -domain using a polyphase notation is given by:

$$\mathbf{y}_p(z) = \mathbf{G}_p(z^{\mathbf{D}}) \cdot \mathbf{H}_p(z^{\mathbf{D}}) \cdot \mathbf{x}_p(z^{\mathbf{D}})$$

¹For matrix and vector algebraic notations used in the following equations, please refer to the appendix A

In this equation, x_p denotes the signal in the polyphase domain. Polyphase decomposition not only enables a parallel implementation of the algorithm parallel but also simplifies the filter design process, which leads to easier understanding.

Kovacevic [6], proves that:

- Alias cancellation is achieved if and only if \mathbf{p}_i is the left eigenvector of the product $\mathbf{G}_p \mathbf{H}_p$
- Perfect reconstruction is achieved if and only if the eigenvalue associated with \mathbf{p}_i is a monomial: z^{-k}
- Perfect reconstruction with an FIR filter is achieved if and only if the determinant of the polyphase matrix is a monomial: $\det \mathbf{H}_p(z) = z^{-k}$

4.1 Polyphase Analysis

Using our down-sampling matrix of Section 3.2 we experience a data reduction by a factor of 4. Hence $N = 4$ for this particular case of a BCC down-sampling matrix. Therefore, there are going to be four polyphase components in the signal as well as our filters:

$$\begin{aligned} h_i(n_1, n_2, n_3) &= h(\mathbf{D}\mathbf{n} + \mathbf{k}_i) \\ h_0(n_1, n_2, n_3) &= h(-n_1 - n_3, n_1 - n_3, -n_1 + 2n_2 + n_3) \\ h_1(n_1, n_2, n_3) &= h(-n_1 - n_3, n_1 - n_3, -n_1 + 2n_2 + n_3 + 1) \\ h_2(n_1, n_2, n_3) &= h(-n_1 - n_3 - 1, n_1 - n_3, -n_1 + 2n_2 + n_3) \\ h_3(n_1, n_2, n_3) &= h(-n_1 - n_3 - 1, n_1 - n_3, -n_1 + 2n_2 + n_3 + 1) \end{aligned}$$

The transpose of our down-sampling matrix D is:

$$\mathbf{D}^t = \begin{bmatrix} -1 & 1 & -1 \\ 0 & 0 & 2 \\ -1 & -1 & 1 \end{bmatrix}$$

Using the algorithm discussed in Section 3.1 we can derive the vectors representing the cosets of \mathbf{D}^t :

$$\mathbf{k}_0 = \begin{bmatrix} 0 \\ 0 \\ 0 \end{bmatrix}, \mathbf{k}_1 = \begin{bmatrix} 0 \\ 1 \\ 0 \end{bmatrix}, \mathbf{k}_2 = \begin{bmatrix} -1 \\ 1 \\ 0 \end{bmatrix}, \mathbf{k}_3 = \begin{bmatrix} 0 \\ 0 \\ -1 \end{bmatrix}$$

4.2 Filter Design

We have all the necessary information to define filters of a perfect reconstruction filter bank. The family of filters that can be designed for non-separable wavelets can be studied in detail. The non-separability brings about attractive properties that does not exist with separable methods. For instance, for any filter (other than Haar filters) the conditions of linear phase and orthogonality cannot coexist in a separable solution. However, in the non-separable case, one can design filters that are both orthogonal and have linear phase [6].

In [6] they design various families of orthogonal and linear phase non-separable wavelets for two-channel subsampling. In this paper we examine the Haar filter² in the non-separable scheme using four channel subsampling since $\det D = 4$. The low-pass Haar filter is simply averaging the phases of the signal. The high pass filters encode the error from linearly predicting each of the phases with the average. This analogy is formally discussed in lifting schemes [[14] [16] [15]]. In the traditional case of down-sampling by two,

²In this paper we limit ourselves to Haar filters for the simplicity of the filter construction. Higher-order filters will further improve our results. However, we found that even Haar filters result in superior down-sampled data sets.

the one dimensional low-pass and high-pass Haar filter results in the following polyphase representation:

$$\mathbf{h0}_p(z) = 1/2 \begin{bmatrix} 1 \\ 1 \end{bmatrix}, \mathbf{h1}_p(z) = 1/2 \begin{bmatrix} 1 \\ -1 \end{bmatrix}$$

The polyphase matrix for the analysis bank is:

$$\mathbf{H}_p(z) = 1/2 \begin{bmatrix} 1 & 1 \\ 1 & -1 \end{bmatrix}$$

For multidimensional signal processing we can extend the idea of linear prediction and the prediction errors for the filter design problem. For BCC subsampling with four phases, we would need to partition the frequency distribution of the signal into four bands, hence we design four bandpass filters as:

$$\begin{aligned} \mathbf{h0}_p(z) &= 1/4 \begin{bmatrix} 1 \\ 1 \\ 1 \\ 1 \end{bmatrix}, \mathbf{h1}_p(z) = 1/4 \begin{bmatrix} 3 \\ -1 \\ -1 \\ -1 \end{bmatrix} \\ \mathbf{h2}_p(z) &= 1/4 \begin{bmatrix} -1 \\ 3 \\ -1 \\ -1 \end{bmatrix}, \mathbf{h3}_p(z) = 1/4 \begin{bmatrix} -1 \\ -1 \\ 3 \\ -1 \end{bmatrix} \end{aligned}$$

Hence, the polyphase matrix for the analysis bank can be written:

$$\mathbf{H}_p(z) = 1/4 \begin{bmatrix} 1 & 1 & 1 & 1 \\ 3 & -1 & -1 & -1 \\ -1 & 3 & -1 & -1 \\ -1 & -1 & 3 & -1 \end{bmatrix} \quad (10)$$

resulting in the following inverse for the synthesis polyphase matrix:

$$\mathbf{G}_p(z) = \begin{bmatrix} 1 & 1 & 0 & 0 \\ 1 & 0 & 1 & 0 \\ 1 & 0 & 0 & 1 \\ 1 & -1 & -1 & -1 \end{bmatrix} \quad (11)$$

which satisfy all of the three conditions in Section 4 for alias cancellation and perfect reconstruction with FIR filters, since $\mathbf{G}(z) \cdot \mathbf{H}(z) = \mathbf{I}$, where \mathbf{I} denotes the identity matrix.

5 IMPLEMENTATION

In this section we discuss the algorithm developed for polyphase decomposition and Haar wavelet transform for the BCC subsampling matrix. Also, we will discuss the rendering methods that were used to obtain images of the datasets subsampled by our method.

5.1 Filter Bank

The implementation of our filter bank is considerably simplified by the polyphase decomposition theory that was discussed in Section 4. There are two main steps that are involved in the analysis section of the filter bank: Polyphase Decomposition, Filtering.

The polyphase decomposition algorithm is simply a vector and matrix division arithmetic once we know the coset vectors of the subsampling matrix.

The top level polyphase decomposition algorithm for subsampling matrix \mathbf{D} is as follows:

```

 $N \leftarrow \det \mathbf{D}$ 
for each  $[x, y, z]$  in the volume do
   $[\mathbf{q}, \mathbf{r}] \leftarrow \text{DIVIDE}([x, y, z]', \mathbf{D})$ 
for each  $i \leftarrow 0 \dots N - 1$  do

```

```

if  $r == \text{Coset}[i]$  then
   $\text{Phase}[i](q) \leftarrow \text{volume}(x, y, z)$ 
  break
end if
end for
end for

```

Also, the division algorithm is application of Cramer's rule:

```

function  $[q, r] \leftarrow \text{DIVIDE}(n, D)$ 
 $N \leftarrow |\det D|$ 
 $q1 \leftarrow \det [n \mid D(:, 2) \mid D(:, 3)]$ 
 $q2 \leftarrow \det [D(:, 1) \mid n \mid D(:, 3)]$ 
 $q3 \leftarrow \det [D(:, 1) \mid D(:, 2) \mid n]$ 
 $r \leftarrow \text{mod}([q1q2q3]', N)$ 
 $q \leftarrow ([q1q2q3]' - r)/N$ 
 $r \leftarrow D \times r/N$ 

```

Once the original volume decomposed into its four phases, we can obtain the various bands of the analysis section by multiplying the polyphase vector, by the polyphase matrix developed in Section 4.2. The following piece of code performs the Haar decomposition:

```

function  $\text{Band} \leftarrow \text{HAAR}(\text{Phase})$ 
 $\text{Band}[0] \leftarrow 1/4 \sum_{i=1}^4 \text{Phase}[i]$ 
 $\text{Band}[1] \leftarrow \text{Phase}[0] - \text{Band}[0]$ 
 $\text{Band}[2] \leftarrow \text{Phase}[1] - \text{Band}[0]$ 
 $\text{Band}[3] \leftarrow \text{Phase}[2] - \text{Band}[0]$ 

```

Basically, the function *HAAR* averages the phases and stores the average in band 0. The other three bands are the details (wavelet coefficients) which are the error of predicting the phases from their average. The synthesis of the filter bank is similarly implemented in the reverse order.

5.2 Rendering Method

In order to evaluate the quality of our novel down-sampling method, we compare our method with a traditional separable method. The separable method applies a filtering and downsampling step in each coordinate axis independently. In order to have a fair comparison we create a downsampled version of the data with the same number of samples, i.e. on forth of the original samples. Hence we have to downsample by a factor of $\sqrt[3]{4}$ in each direction. The filter we are using is linear interpolation along the three axis; this choice of filter is only fair for comparison with the Haar filtering that is used for the non-separable subsampling.

In order to compare the downsampled data obtained from BCC downsampling and separable Cartesian downsampling, we used several methods to render the resulting data. We used the splatting method developed by [8] and the hardware accelerated texture slice rendering method in [10]. We also developed our own raycasting program in which we used a spherical kernel for interpolation purposes on the BCC lattice and the Cartesian lattice. While the results of the comparison between BCC and Cartesian subsampled data are consistent across different rendering methods, none of the existing methods are able to fully take advantage of the high frequencies existing in the BCC subsampled data. In order to do proper interpolation in the BCC lattice, and hence to obtain more accurate renditions of BCC sampled data, one needs to find the appropriate interpolation filter that cuts the voronoi cell of the frequency transform of the BCC lattice (which happens to be an FCC lattice). This problem remains to be studied.

For our purposes we simply use a linear approximation, i.e. we use a spherical extension of the cone filter. The radial filter that we use is described by Equation 12

$$h(x, y, z) = \max(0, \text{RADIUS} - \sqrt{x^2 + y^2 + z^2}) \quad (12)$$

The *RADIUS* of the kernel is dependent on the lattice that it is resampling. The extent of the radial kernel for the BCC lattice is chosen to be $R_{bcc} = 2$ as that is the radius of the rhombic dodecahedron surrounding a BCC lattice point. However, the volume of the frequency domain representation of the data on the BCC lattice is $\sqrt{2}$ larger than the volume of the spectrum of the Cartesian data [8]. We also know that the radius of the kernel in space domain has an inverse relation with the radius of its support in frequency domain. Therefore, to be fair to the Cartesian the radial kernel chosen for the Cartesian rendering is set to be $R_{cc} = 2\sqrt[3]{2}$.

6 RESULTS

In this section we will present the images obtained from our raycasting method discussed in Section 5.2. We subsampled several datasets³ to get conclusive results on the superiority of the images obtained by our BCC subsampling method.

The renditions of the original volumes are demonstrated in Figure 4

The downsampled versions of these datasets were computed using the algorithms discussed in the Section 5.1. The images in the Figures 1, 5 and 6 show the images of the rendered subsampled datasets. The image on the left is the Cartesian subsampling method and the figure on the right is the BCC subsampled dataset.

For the Engine dataset in Figure 1 the overall specular contrast of the BCC image suggests the higher frequencies preserved by the BCC subsampling method. Moreover, the details are visible around the circular areas of the pistons. Similarly, on the UNC Brain dataset in Figure 6, it is interesting to notice that the BCC images is slightly more detailed as predicted; this is specially noticeable on the areas around the eyebrows, lips and on the cheeks.

The original hydrogen atom model in Figure 4 has some high frequencies (mostly artifacts) due to the reconstruction process which was used to create it. The fidelity of the BCC subsampling method is shown in Figure 5 as all of those details are lost in the left image and some of the high frequencies are preserved on the right image.

7 CONCLUSIONS AND FUTURE WORK

We have examined and developed the mathematical framework for designing and developing filter bank theory for the BCC sampling lattice. This is an important step towards making the efficient BCC lattice a viable alternative to the commonly used Cartesian sampling systems.

We have successfully created a BCC sampling matrix and the corresponding filter bank for Haar wavelets, which resulted in downsampled version of an original Cartesian data set of superior fidelity over comparable separable (Cartesian) downsampling methods. One strength of our method is that it can be directly applied to an existing Cartesian lattice without any apriori resampling operations. Furthermore our method is computationally more efficient than comparable separable downsampling methods.

There are various areas that need further investigation and study. Designing higher order wavelets than the Haar wavelets is a challenging task. There have been studies of higher order wavelets for non-separable wavelet transforms for the case of two-channel subsampling [3] [6]; however, this area is not well studied for the case of four-channel subsampling that is the case for BCC subsampling ($\det D = 4$) as discussed in this paper. In this paper we have demonstrated how to obtain the smallest in the family of non-separable four-channel wavelets. However, comparing higher order wavelets with the corresponding order of wavelets in the separable

³The original datasets are obtained from www.volvis.org

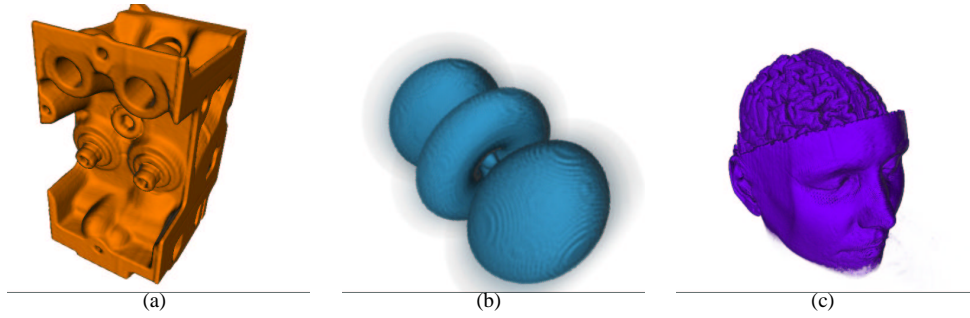


Figure 4: Original datasets: (a) Engine(256 × 256 × 128) (b) Hydrogen Atom (128 × 128 × 128) (c) UNC Brain (256 × 256 × 145)

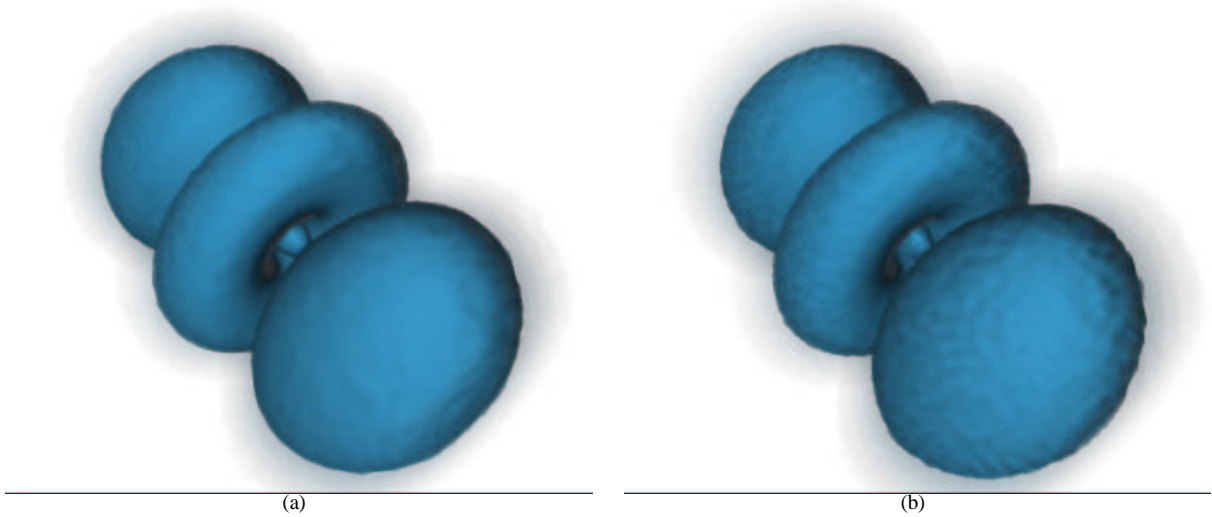


Figure 5: Hydrogen Atom, separable subsampling (left) and our non-separable subsampling(right)

schemes would give rise to a wider range of options when selecting wavelets for BCC lattices.

In terms of wavelet based compression techniques [11], further investigation is required to determine how the optimality of the underlying sampling lattice affects the quality and the ratio of the compression. The existing wavelet based denoising techniques should be examined for possible advantages, when applied to the non-separable scheme.

Another research direction that demands closer attention is the issue of interpolation when trying to display BCC sampled data. Investigating various families of filters on the Voronoi cell of the reciprocal of the BCC lattice would result in more efficient filters that will in turn reveal more advantages of the BCC sampled data.

A NOTATIONS

In this appendix we establish the mathematical notation used throughout the paper. The notation closely follows that used in [6].

- Boldface lower (upper) case letters denote vectors (matrices).
- Raising an n-dimensional complex vector $z = [z_1 \dots z_n]^t$ to an n-dimensional integer vector $k = [k_1 \dots k_n]^t$ is a scalar

which denotes componentwise operations:

$$z^k = z_1^{k_1} z_2^{k_2} \dots z_n^{k_n}$$

- \mathcal{Z}^n denotes the space of n-dimensional integer vectors.
- The Z -transform of a discrete sequence $h(k) = h(k_1, \dots, k_n)$ is defined as:

$$H(z) = \sum_{k \in \mathcal{Z}^n} h(k) z^{-k}$$

- Raising a vector z to a matrix power D is defined as:

$$z^D = [z^{d_1}, z^{d_2}, \dots, z^{d_n}]^t$$

where d_i is the i^{th} column of the matrix D .

REFERENCES

- [1] Hamish Carr, Thomas Theußl, and Torsten Möller. Isosurfaces on Optimal Regular Samples. *Joint EUROGRAPHICS and IEEE TCVG Symposium on Visualization*, May 2003.

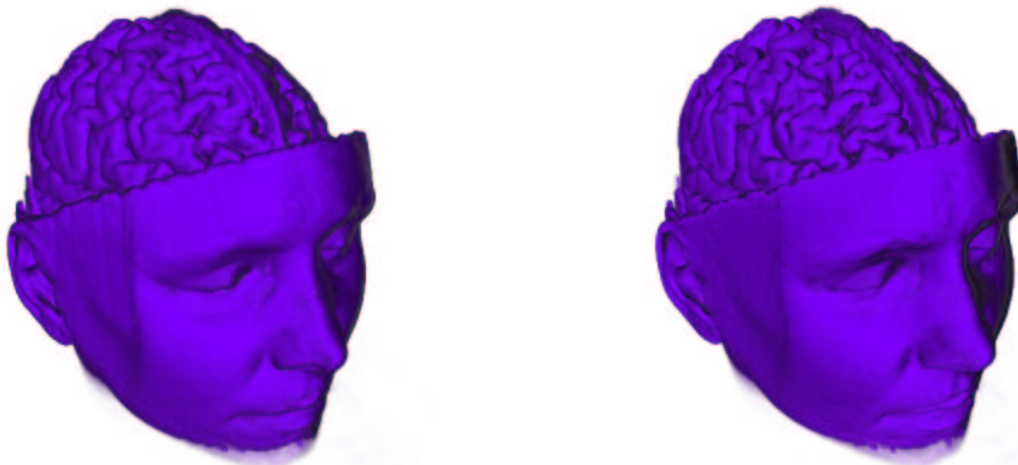


Figure 6: UNC Brain, separable subsampling (left) and our non-separable subsampling(right)

- [2] J.H. Conway and N.J.A. Sloane. *Sphere Packings, Lattices and Groups*. Springer, 3rd Edition, 1998.
- [3] Todor Cooklev. *Regular Perfect-Reconstruction Filter Banks and Wavelet Bases*. Ph.d dissertation, Tokyo University of Technology, Tokyo, Japan, 1995.
- [4] Ingrid Daubechies. Ten lectures on wavelets. *IEEE Transactions on Information Theory*, 17(10):939–954, Mar. 1992.
- [5] D.E. Dudgeon and R.M. Mersereau. *Multidimensional Digital Signal Processing*. Prentice-Hall, Inc., Englewood-Cliffs, NJ, 1984.
- [6] Jelena Kovacevic and Martin Vetterli. Nonseparable multi-dimensional perfect reconstruction filter banks and wavelet bases for \mathcal{R}^n . *IEEE Transactions on Information Theory*, 17(10):939–954, Mar. 1992.
- [7] J. Kovačević and M. Vetterli. FCO sampling of digital video using perfect reconstruction filter banks. *IEEE Trans. Image Proc.*, 2(1):118–122, January 1993.
- [8] Thomas Theußl, Torsten Möller, and Meister Eduard Gröller. Optimal regular volume rendering. *IEEE Visualization*, 17(10):939–954, Oct. 2001.
- [9] N. Neophytou and K. Mueller. Space-time points splatting in 4d. *Symposium on Volume Visualization and Graphics 2002*, 17(10):97–106, October 2002.
- [10] Niklas Röber, Markus Hadwiger, Alireza Entezari, and Torsten Möller. Texture based volume rendering of hexagonal data sets. *Tech. Report*, 2003.
- [11] Jon Rogers and Pamela Cosman. Wavelet zerotree image compression with packetization. *IEEE Signal Processing Letters*, 17(10):939–954, Mar. 2002.
- [12] Eero P. Simoncelli. Noise Reduction Via Bayesian Wavelet Coring. *IEEE Transactions on Information Theory*, 17(10):939–954, Mar. 1992.
- [13] E.P. Simoncelli and E.H. Adelson. Nonseparable extensions of quadrature mirror filters to multiple dimensions. *Proceedings of IEEE, Special Issue on Multi-dimensional Signal Processing*, 78(4):652–664, April 1990.
- [14] W. Sweldens. The lifting scheme: A new philosophy in biorthogonal wavelet constructions. In A. F. Laine and M. Unser, editors, *Wavelet Applications in Signal and Image Processing III*, pages 68–79. Proc. SPIE 2569, 1995.
- [15] W. Sweldens. Wavelets and the lifting scheme: A 5 minute tour. *Z. Angew. Math. Mech.*, 76 (Suppl. 2):41–44, 1996.
- [16] W. Sweldens. The lifting scheme: A construction of second generation wavelets. *SIAM J. Math. Anal.*, 29(2):511–546, 1997.
- [17] P.P. Vaidyanathan. *Multirate Systems and Filter Banks*. Signal Processing. Prentice Hall, Englewood Cliffs, New Jersey 07632, 1993.
- [18] M. Vetterli, J. Kovačević, and D. J. LeGall. Perfect reconstruction filter banks for HDTV representation and coding. *Image Communication, special issue on HDTV*, 2(3):349–364, October 1990. Invited paper.
- [19] M. Vetterli, J. Kovačević, and D. J. LeGall. *Signal Processing of HDTV, II*, chapter Perfect Reconstruction Filter Banks for HDTV Representation and Coding. Elsevier, 1990.